Physica A 594 (2022) 127015

Contents lists available at ScienceDirect

Physica A

journal homepage: www.elsevier.com/locate/physa

Approach to failure through record breaking avalanches in a heterogeneous stress field

Viktória Kádár [a], Zsuzsa Danku [a], Gergő Pál [a,b], Ferenc Kun [a,b,*]

[a] University of Debrecen, Faculty of Science and Technology, Doctoral School of Physics, Department of Theoretical Physics, P.O. Box 400, Debrecen, H-4002, Hungary

[b] Institute of Nuclear Research (Atomki), Poroszlay út 6/c, Debrecen, H-4026, Hungary

ARTICLE INFO

Article history:
Received 4 July 2021
Received in revised form 19 January 2022
Available online 4 February 2022

Keywords:
Fracture
Crackling noise
Ultimate failure
Fiber bundle model
Record statistics
Forecasting

ABSTRACT

We study how the competition of the disordered local strength and of the evolving inhomogeneous stress field affects the evolution of the series of breaking avalanches accompanying the fracture of heterogeneous materials. To generate fracture processes, we use a fiber bundle model of localized load sharing where the degree of strength disorder is controlled by varying two parameters of the distribution of the breaking threshold of fibers. Analyzing the record statistics of avalanches of breaking fibers, we demonstrate that both for low and high disorders the series of crackling events remains stationary until global failure making the collapse of the system unpredictable. Based on computer simulations, we determine a region of the parameter plane of strength disorder where global failure is preceded by an accelerating breaking activity. We show that the record avalanche with the longest lifetime can be used to identify the onset of acceleration of the fracture process towards the catastrophic failure. Comparison of the results to their equal load sharing counterparts reveals that the accelerating regime is shorter than in case of a homogeneous stress field due to the higher degree of brittleness of the system caused by stress localization.

1. Introduction

Under a slowly increasing mechanical load the fracture of heterogeneous materials proceeds in bursts which generate acoustic noise, and hence, can be recorded by acoustic emission techniques [1–5]. The time series of such crackling events provides a deep insight into the dynamics of fracturing and can be exploited to forecast the imminent catastrophic collapse of the evolving system [1,6]. Forecasting fracture driven failure has an utmost importance for natural catastrophes like snow and stone avalanches, landslides [6], and earthquakes [7,8], as well as, for engineering constructions [9]. The size of bursts has strong fluctuations due to materials' disorder, however, its statistics has been found to obey a robust power law behavior over a broad range of event sizes for a wide variety of materials [1,2,2–4]. As the external load increases, under certain conditions the dynamics of fracturing accelerates in the vicinity of global failure which is indicated e.g. by the increasing average burst size and deformation rate [1,6,10]. One of the main motivations of fracture studies is to identify signatures of the imminent failure which can be exploited for forecasting. The failure forecast methods (FFM) rely on the analogy of fracture and phase transitions, i.e. time-to-failure power laws characterizing the accelerating phase are used to predict the point of global failure [7,10–12].

* Corresponding author at: University of Debrecen, Faculty of Science and Technology, Doctoral School of Physics, Department of Theoretical Physics, P.O. Box 400, Debrecen, H-4002, Hungary.
E-mail address: ferenc.kun@science.unideb.hu (F. Kun).

https://doi.org/10.1016/j.physa.2022.127015
0378-4371/

Recently, we have shown in a fiber bundle model (FBM) of long range load sharing that based on the record statistics of crackling events a clear signal of the onset of acceleration towards global failure can be obtained [13]. Records of the sequence of breaking avalanches are those events which have a magnitude greater than any previous event. From a practical point of view they have the advantage that they are easy to identify above the noisy background both in laboratory and field measurements. For sequences of independent identically distributed random variables (IID) the statistics of records has been found to exhibit universal features, independent of the underlying distribution of individual events [14,15]. We demonstrated that deviations from the IID behavior in the sequence of crackling avalanches reveals interesting trends and correlations which can be used to identify early signatures of the impending catastrophic failure [13,16]. However, these studies were limited to equal load sharing in the fiber bundle model where the stress field remains homogeneous during the entire fracture process. In fracturing materials high stress concentration builds up in the vicinity of cracks which makes the stress field inhomogeneous and has a strong effect on the fracture process.

To understand how the inhomogeneous stress field affects the sequence of breaking avalanches, in particular, the evolution of the sequence as the system approaches failure, here we consider the limiting case of short range load sharing in the fiber bundle model and study the emerging crackling activity using record statistics. We generate fracture processes by means of a fiber bundle model where fibers are organized on a square lattice and load is redistributed over the intact nearest neighbors of broken fibers. As the external load increases in the model, the fracture process is driven by the competition of the evolving inhomogeneous stress field and of the disordered strength of fibers. Computer simulations showed that for low strength disorder the stress concentration dominates the fracture process making the overall response of the system highly brittle, i.e. the system evolves through breaking avalanches, however, no acceleration of the process, and hence, no signal of the imminent failure can be detected. In the limit of very high disorder again a stationary evolution is obtained without the possibility of forecasting. As the main outcome we show that there exists a range of disorder where accelerated record breaking precedes failure and the onset of acceleration can be used as an early warning of the impending failure.

2. Breaking avalanches in a fiber bundle model of localized load sharing

In our study we consider a bundle of N parallel fibers which are organized on a square lattice of side length L, where $N = L^2$ holds [17–20] (for an illustration see Fig. 1(*a*)). Individual fibers are assumed to have a linearly elastic behavior up to a threshold strain ε_{th} at which they break irreversibly. The Young modulus E has a fixed value $E = 1$ for all the fibers, however, the strength ε_{th} is a random variable sampled from a probability distribution $p(\varepsilon_{th})$. For the functional form of $p(\varepsilon_{th})$ we consider a power law

$$p(\varepsilon_{th}) \sim \varepsilon_{th}^{-(1+\mu)} \tag{1}$$

over a finite range $\varepsilon_{min} \leq \varepsilon_{th} \leq \varepsilon_{max}$, where the lower bound is fixed $\varepsilon_{min} = 1$. The random failure threshold of fibers represents the fluctuations of the local strength of material elements caused by the presence of flaws, micro-cracks, or by any imperfection due to the fabrication process. The threshold distribution Eq. (1) has the advantage that the amount of strength disorder can be controlled by varying the upper bound ε_{max} of strength values in the range $\varepsilon_{min} \leq \varepsilon_{max} < \infty$, and the exponent μ of the distribution $0 < \mu < 1$. The bundle is subject to a quasi-static loading, which is carried out by increasing the external load σ to induce the breaking of a single fiber. When all the fibers are intact, they keep the same load, hence, the weakest fiber breaks first. After a fiber breaks, its load has to be redistributed over the remaining intact fibers. In FBM studies of fracture processes two limiting cases of load sharing are typically considered both with practical relevance: In the case of equal load sharing (ELS) the load of the broken fiber is equally shared by all the intact fibers irrespective of their distance from the failed one. ELS has the consequence that no stress fluctuations emerge in the system which makes it possible to obtain important characteristic quantities of the model in closed analytic forms [18,21,22]. Localized load sharing (LLS) realizes the opposite limit redistributing the load equally over the intact nearest neighbors of the broken fiber in the lattice [23–26]. LLS results in a high stress concentration around broken fibers which in turn has a strong effect on the evolution of the fracture process. After load redistribution, the enhanced load of intact fibers may induce further breakings which is then followed again by a load redistribution. As a consequence, through the repeated steps of breaking and load redistribution, a single fiber failure can trigger an entire avalanche of breaking events whose size Δ is defined as the number of fibers breaking in the avalanche.

Since the stress field is homogeneous, in the ELS case the strength disorder of fibers controls the fracture process. We have shown analytically that at each value of the exponent μ there exists a threshold value of the upper cutoff ε_{max}^c below which $\varepsilon_{max} < \varepsilon_{max}^c$ the system exhibits a perfectly brittle behavior, i.e. the first breaking fiber triggers a catastrophic avalanche which results in immediate failure of the entire bundle [27,28]. Above the critical cutoff $\varepsilon_{max} > \varepsilon_{max}^c$ the distribution $p(\varepsilon_{th})$ is sufficiently broad so that avalanches have the opportunity to stop. Hence, in this parameter range the fracture process is accompanied by a sequence of avalanches making the response of the bundle quasi-brittle. Analytical calculations and computer simulations have revealed that in the limit of an infinite cutoff $\varepsilon_{max} \to \infty$ the fracture process remains stable during the entire loading process in the sense, that no catastrophic avalanche occurs and the overall response of the bundle shows analogies to ductile failure. For ELS, the phase boundary $\varepsilon_{max}^c(\mu)$ separating the perfectly brittle and quasi-brittle phases can be obtained analytically [27–29]

$$\varepsilon_{max}^c(\mu) = \frac{\varepsilon_{min}}{(1-\mu)^{1/\mu}}. \tag{2}$$

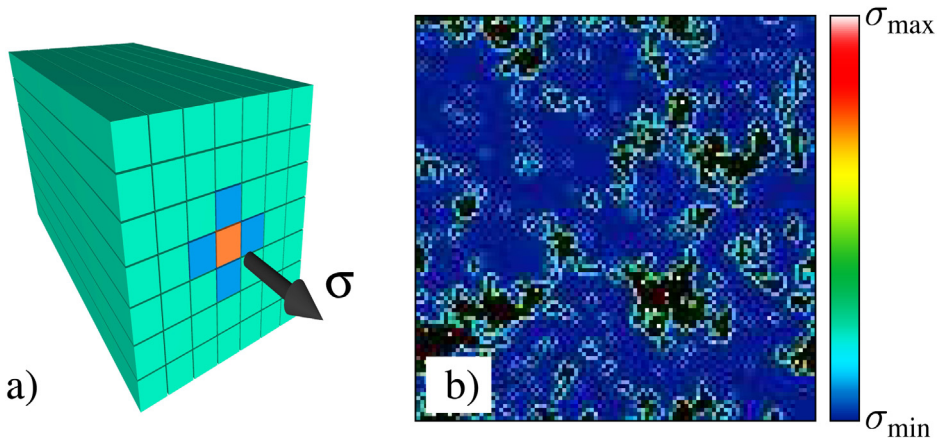

Fig. 1. (a) Schematic representation of the model construction: parallel fibers are arranged on a square lattice. The bundle is loaded parallel to the fibers' direction. The colored fibers illustrate that the load of a broken fiber is equally shared by its (at most four) nearest neighbors. (b) Stress distribution in a relatively small fiber bundle of size $L = 101$. Localized load sharing results in a high stress concentration so that fibers along the perimeter of broken clusters (cracks in the model) experience an elevated load. The larger the crack is, the higher stress accumulates on perimeter fibers giving rise to an evolving inhomogeneous stress field.

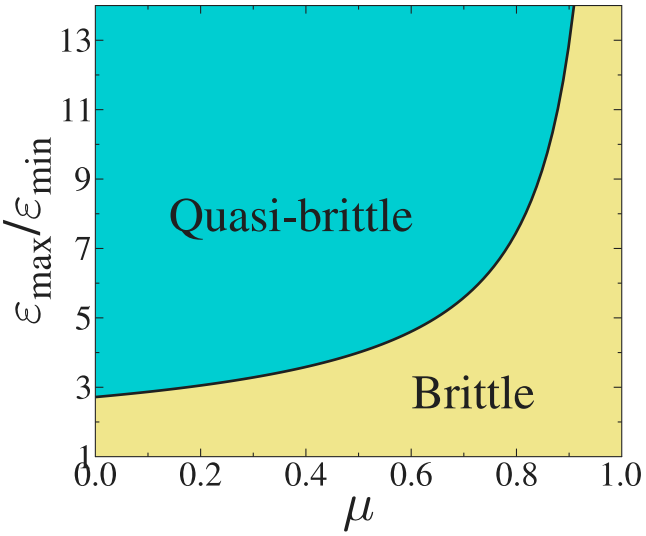

Fig. 2. Phase diagram of the ELS FBM with the threshold disorder Eq. (1) on the $\mu - \varepsilon_{max}$ plane. The continuous line represents the phase boundary given by Eq. (2). Ductile behavior is obtained in the limit $\varepsilon_{max} \to \infty$.

The phase diagram of Fig. 2 provides an overview of the different types of responses of ELS FBMs with the fat tailed strength disorder Eq. (1) on the $\mu - \varepsilon_{max}$ parameter plane. Note that for $\mu > 1$ the system is in the perfectly brittle phase at any cutoff values, hence, the critical value of the strength exponent μ_c at the infinite cutoff is $\mu_c = 1$. To characterize the cutoff of the distributions it is instructive to introduce the relative distance from the phase boundary $\lambda = \varepsilon_{max}/\varepsilon^c_{max}(\mu) - 1$, which can take values between 0 and ∞ to cover the quasi-brittle and ductile phases. To classify LLS simulations we start from the ELS phase diagram (Fig. 2) selecting $\mu - \lambda$ parameter pairs for computer simulations and compare the results to their ELS counterparts. The phase boundary between the perfectly brittle and quasi brittle behaviors was obtained analytically for the limit of infinite system size, however, for finite systems fluctuations may occur, which makes the transition less sharp. In fracture studies scale free disorder distributions were first introduced in Ref. [30] with the additional freedom that instead of a power law tail towards the large thresholds, a power law decrease towards zero strength can also be considered with a finite upper cutoff. Recently, it has been shown that the nature of the brittle to quasi brittle transition is different in the two cases [31]. Following our former studies, here we consider only Eq. (1) for the threshold distribution to be able to compare our LLS results to their ELS counterparts [13].

In an LLS FBM fibers breaking in an avalanche form a connected cluster, which can be considered as a crack in the model. Hence, the avalanche stops when all intact fibers along the perimeter of the cluster can sustain the load

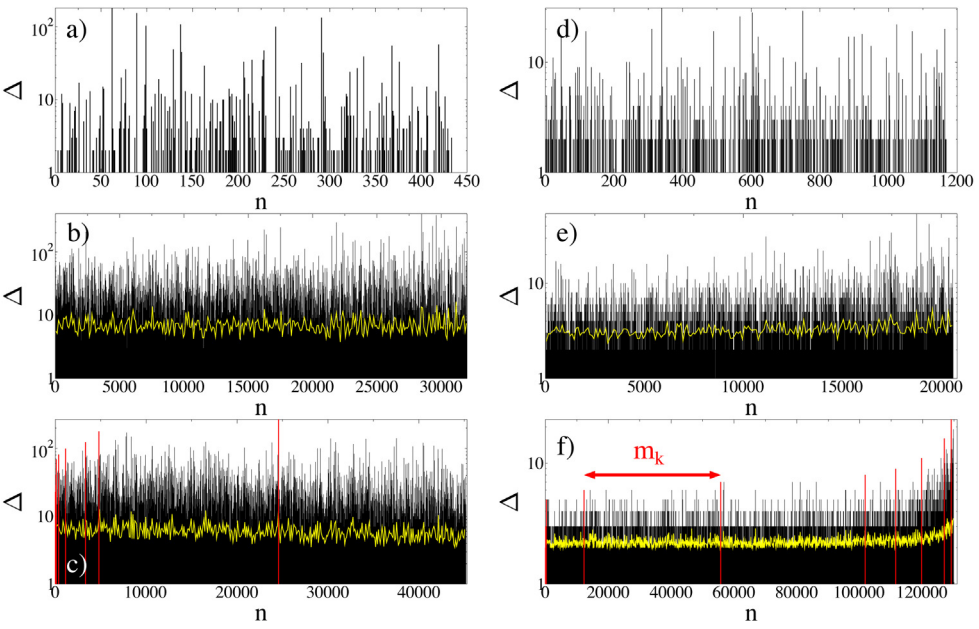

Fig. 3. Sequence of breaking avalanches up to failure at two different disorder exponents $\mu = 0.8$ (left column) and $\mu = 0.1$ (right column) varying the cutoff strength λ in broad ranges: (a) 1.5, (b) 50, (c) 10^3, (d) 1.5, (e) 50, (f) 10^6. The size of avalanches Δ_n is presented as a function of their order number n. The yellow line indicates the moving average of the burst size considering 50 consecutive events. In (c) and (f) record size avalanches are highlighted in red. (f) also demonstrates the definition of the lifetime m_k of records.

accumulated from the interior of the cluster. As the external load increases, new cracks nucleate and the existing ones gradually grow, hence, the stress field on the surviving intact fibers becomes more and more inhomogeneous. This is illustrated in Fig. 1 for a lattice of size $L = 101$, where fibers are colored according to the load they keep. The accumulated load on perimeter fibers of broken clusters makes them more prone to breaking. It is an important characteristics of our model that it has two sources of disorder, i.e. the random strength of fibers, which is quenched, and the stress field which evolves as fibers breaks. The degree of strength disorder can be controlled by varying the parameters μ and λ of the threshold distribution $p(\varepsilon_{th})$, while the stress disorder is determined by the range of load sharing, which is fixed to nearest neighbors. The competition of the two disorders leads to a complex evolution of the fracture process through avalanches of fiber breakings.

Our goal is to give a quantitative characterization of the series of breaking avalanches, in particular, to analyze if signatures of the impending global failure could be pointed out in the avalanche sequence when stress concentrations are present in the system. We performed computer simulations on a square lattice of size $L = 401$, with periodic boundary conditions in both directions, generating quasi-static fracture processes varying the upper bound λ and the exponent μ of the threshold distribution in broad ranges. To understand how the localized load redistribution and the emerging inhomogeneous stress field affect the evolution of the system, we compare the results to the case of equal load sharing, where the stress field remains always homogeneous. To analyze the sequence of breaking avalanches we apply the methods of record statistics which have proven powerful in fracture studies [13,16,32,33]. In the data analysis, quantities of interest were averaged over $K = 2000$ samples for each parameter set.

3. Evolution of the sequence of breaking avalanches

Avalanches of breaking fibers generated under a slowly increasing external load are analogous to the acoustic outbreaks observed in real measurements. The acceleration of the crackling activity forms the basis of failure forecast methods [10,34]. Hence, it is a crucial question how the interplay of materials' disorder and the inhomogeneous stress field affects the acceleration preceding global failure. Fig. 3 presents the sequence of avalanches of LLS bundles by plotting the size of bursts Δ_n as a function of their order number $n = 1, \ldots, n_{max}$ up to global failure for several parameter sets. Here n_{max} denotes the total number of avalanches up to failure. It can be observed that for a high exponent $\mu = 0.8$ where the threshold distribution Eq. (1) rapidly decreases (Fig. 3(a, b, c)) the event series remains nearly stationary at all cutoff values λ, i.e. no sign of acceleration can be inferred by visual inspection. At a significantly lower exponent $\mu = 0.1$ where the strength distribution decays slowly (Fig. 3(d, e, f)) the same behavior is observed for low λ values close to the phase boundary of brittle failure (Fig. 3(d)), i.e. fracture of the bundle evolves in a stationary way where the avalanche size Δ fluctuates about an average value $\langle\Delta\rangle$. However, for higher cutoff values (Fig. 3(f)) the avalanche size tends to increase

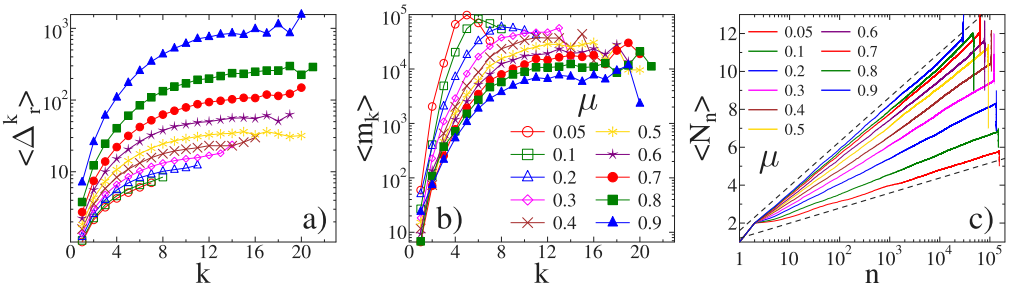

Fig. 4. Average size $\langle \Delta_r^k \rangle$ (a) and average lifetime $\langle m_k \rangle$ (b) of records as a function of their rank k for an infinite upper cutoff of fibers' strength $\lambda = \infty$ for the same exponents μ. Apart from fluctuations at the highest ranks, both quantities increase monotonically with k. (c) The average number of records $\langle N_n \rangle$ which occurred up to the event number n. The dashed straight lines represent logarithmic curves with slopes $B = 0.3$ and $B = 1.1$.

in the vicinity of global failure. This acceleration of the breaking process becomes more pronounced at an even higher cutoff, where the increase of the burst size sets on earlier making the acceleration regime broader.

Our goal is to give a quantitative characterization of the transition from stationary evolution to acceleration as the system approaches failure, while the competition of the strength and stress disorders is controlled by varying the parameters μ and λ.

3.1. Record breaking events in avalanche sequences

To analyze the evolution of the sequence of breaking avalanches we focus on the record size avalanches of the fracture process. A record is an avalanche which has a size Δ_r greater than any previous event. Records are identified by their rank $k = 1, 2, \ldots, k_{max}$, which occurred as the n_kth event of the sequence of avalanches. By definition the first burst of the fracture process is a record with $k = 1$ so that $n_1 = 1$ follows. Starting from the first record all subsequent records can be found as those bursts which break the previous record. It can be observed in Fig. 3 that records form a monotonically increasing sub-sequence of the crackling event series, but the size of records Δ_r^k of a given rank k may still have strong sample-to-sample fluctuations.

As fracture of the bundle proceeds records get broken after a certain number of avalanches which defines the waiting time m_k between consecutive records

$$m_k = n_{k+1} - n_k. \tag{3}$$

The quantity m_k is also called as the lifetime of the kth record. For the last record of rank k_{max} the lifetime is defined as $m_{k_{max}} = n_{max} - n_{k_{max}}$. The definition of records is demonstrated in Figs. 3(c, f), highlighting the record breaking (RB) events of two event series. It can be observed in Fig. 3(c) that for a nearly stationary event sequence only a few records occur $N_n^{tot} = 5$ up to failure in spite of the relatively large number of events $n_{max} \approx 45.000$. When the fracture process accelerates in the vicinity of failure (see Fig. 3(f)) a larger number of records can be identified $N_n^{tot} = 9$. Additionally, it can be inferred that as acceleration sets on record breaking also accelerates indicated by the decreasing lifetime m_k of records.

3.2. Record statistics of avalanches at infinite cutoff strength

It is a great advantage of using record statistics that for sequences of independent identically distributed (IID) random variables several important characteristic quantities of records can be obtained in closed analytical forms. These analytic solutions showed a high robustness of the record statistics of IIDs with quantities being independent of the underlying distribution of individual events. In our study of the evolution of the avalanche sequence of LLS bundles, we use the IID results as a reference which can be expected to well describe the limiting case of the dominance of strength disorder $\lambda \to \infty$. Characteristic quantities of the RB process of this limiting case are illustrated in Fig. 4 for several values of the disorder exponent μ. The figure presents the average size $\langle \Delta_r^k \rangle$ and average lifetime $\langle m_k \rangle$ of consecutive records as a function of their rank k, along with the average number of records $\langle N_n \rangle$ which occurred up to a number n bursts are generated in the evolving system. Of course, the size of records monotonically increases in all cases and tend to saturate for large ranks (Fig. 4(a)). However, it is interesting to note that as μ increases, i.e. the degree of strength disorder decreases, both the size of records at a given rank k and their highest rank k_{max} reaches higher values. It shows that at lower disorder the fracture process is characterized by a more intensive record breaking activity. Since records grow monotonically, it becomes harder and harder to break a new record so that in Fig. 4(b) the lifetime $\langle m_k \rangle$ also monotonically increases apart from some fluctuations at the highest ranks. For higher exponents μ the plateau value of $\langle m_k \rangle$ shifts downward, which indicates the acceleration of record breaking as the strength disorder is lowered.

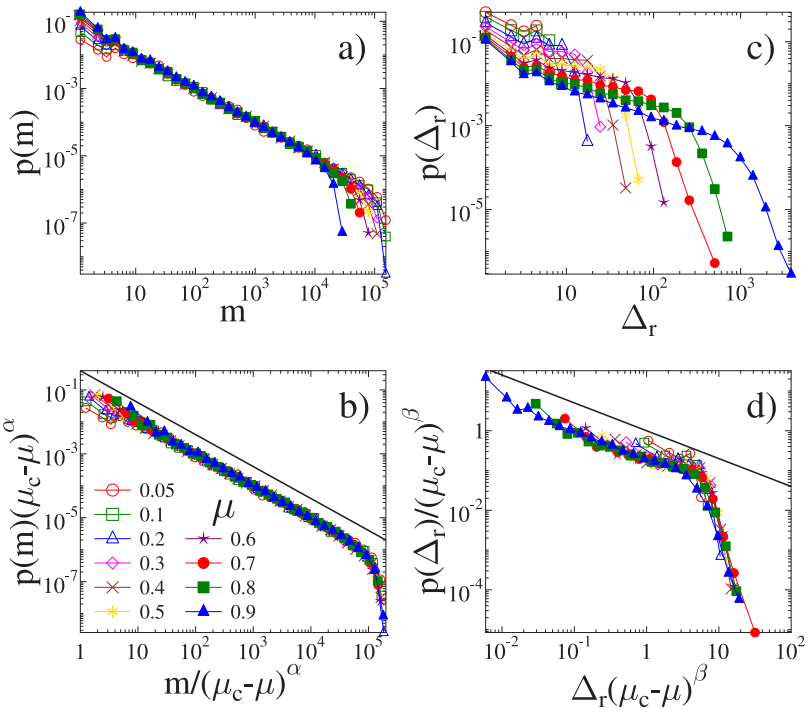

Fig. 5. Probability distribution of the lifetime $p(m)$ (a) and size $p(\Delta_r)$ (c) of records in the LLS FBM at an infinite cutoff strength $\lambda = \infty$. (b) and (d) demonstrates that rescaling both axis with a proper power of the distances from the critical point $\mu_c - \mu$ the distributions obtained at different μ exponents can be collapsed on the top of each other. Best collapse is obtained with the exponents $\alpha = 0.8$ and $\beta = 2.3$, in (b) and (d), respectively. The two straight lines represent power laws of exponent -1 and -0.7 in (b) and (d), respectively.

Fig. 4(*c*) demonstrates that the average number of records $\langle N_n \rangle$ increases logarithmically with the number of events n for all disorder exponents μ considered

$$\langle N_n \rangle = A + B \ln n. \tag{4}$$

The value of A was found to fluctuate between 0.6 and 1.0, while B is an increasing function of μ since at lower disorder (higher μ) a larger number of records occurs up to the same number of avalanches n. Note that the size of records Δ_r^k of a given rank k, their lifetime m_k and the total number of records that occurred up to failure all have sample-to-sample fluctuations. The sample averaging is responsible for the fluctuations of the curves observed at high record ranks in Figs. 4*(a,b)* and at the end of the $\langle N_n \rangle$ curves in Fig. 4(*c*).

A more detailed view on the statistics of records is provided by the probability distribution of the lifetime $p(m)$ and size $p(\Delta_r)$ of records which are presented in Fig. 5(*a*) and Fig. 5(*c*), respectively. At all disorder exponents μ the lifetime distribution exhibits a power law decay

$$p(m) \sim m^{-z}, \tag{5}$$

with the same exponent $z = 1$ which coincides with the corresponding results of IIDs [14,15,35] (see Fig. 5(*a*)). It can be observed that the value of μ only controls the cutoff of the distribution which decreases as the degree of disorder gets reduced. Fig. 5(*b*) demonstrates that rescaling the lifetime distributions with an appropriate power α of the distance from the critical point $\mu_c(\lambda = \infty) = 1$, the distributions obtained at different μ values can be collapsed on the top of each other. Best collapse is obtained with the exponent $\alpha = 0.8$. The size distribution of records $p(\Delta_r)$ is not expected to show a universal behavior since it must depend on the underlying distribution of avalanche sizes $p(\Delta)$. In Fig. 5(*c*) a power law behavior of $p(\Delta_r)$ is evidenced

$$p(\Delta_r) \sim \Delta_r^{-\tau_r}, \tag{6}$$

which is followed by an exponential cutoff. Reducing strength disorder by increasing the exponent μ the functional form of the distribution remains robust, only the cutoff record size Δ_r^{max} shifts to higher values in agreement with the behavior of the average record size in Fig. 4(*a*). Applying the same rescaling transformation as for the lifetime distribution but with a different critical exponent β, the distributions of different μ can be again collapsed on a master curve. Best collapse is achieved in Fig. 5(*d*) with the exponent $\beta = 2.3$. The high quality data collapse of the distributions of the lifetime and

size of records implies the validity of the scaling structures

$$p(m, \lambda = \infty, \mu) = (\mu_c - \mu)^{-\alpha} \Phi(m/(\mu_c - \mu)^{\alpha}), \tag{7}$$

$$p(\Delta_r, \lambda = \infty, \mu) = (\mu_c - \mu)^{\beta} \Psi(\Delta_r(\mu_c - \mu)^{\beta}), \tag{8}$$

where $\mu_c = 1$ and the scaling functions $\Phi(x)$ and $\Psi(x)$ have a power law behavior over a broad range $\Phi(x) \sim x^{-z}$ and $\Psi(x) \sim x^{-\tau_r}$. The two exponents z and τ_r were determined by fitting straight lines in Figs. 5(b, d) $z = 1 \pm 0.05$ and $\tau_r = 0.7 \pm 0.04$. The scaling analysis implies that in the limit of high disorder $\lambda = \infty$ the average values of the longest lifetime $\langle m^{max} \rangle$ and largest size $\langle \Delta_r^{max} \rangle$ both have a power law dependence on the distance from the critical disorder exponent $\mu_c(\lambda = \infty) = 1$ as

$$\langle m^{max} \rangle \sim (\mu_c - \mu)^{\alpha}, \tag{9}$$

$$\langle \Delta_r^{max} \rangle \sim (\mu_c - \mu)^{-\beta}, \tag{10}$$

so that $\langle m^{max} \rangle$ tends to zero, while $\langle \Delta_r^{max} \rangle$ diverges in the limit $\mu \to \mu_c$.

In ELS FBM a similar scaling behavior has been obtained for the probability distribution of the lifetime and size of records, however, with different critical exponents $\tau_r = 1.0$, $\beta = 1.8$, and $z = 1.0$, $\alpha = 1.0$ [13]. The lower value of τ_r and higher value of β in LLS FBM show that stress inhomogeneities give rise to a higher fraction of larger records and a faster divergence of the characteristic record size than the homogeneous stress field. The independence of the value of z from the range of load sharing indicates that in both ELS and LLS cases the strength disorder controlls the breaking process making the avalanche sequence similar to IID sequences. The lower cutoff exponent α of the record lifetime in LLS FBMs implies a slower convergence of the characteristic lifetime to zero as the critical exponent μ_c is approached compared to the ELS case.

It is important to note that the above behavior of the record size, lifetime, and record number is completely consistent with the record statistics of IIDs, showing the high degree of stationarity of the sequence of avalanches in the limit of an infinite upper cutoff of fibers' strength. The results imply that in spite of the stress localization around broken clusters of fibers, the slowly decaying broad distribution of failure thresholds ensures the dominance of strength disorder in the evolution of the fracture process destroying all effects of spatial correlations.

3.3. Record breaking avalanches at finite cutoff strength

As the cutoff strength of fibers λ takes finite values and approaches the phase boundary between the perfectly brittle and quasi-brittle phases from above (see Fig. 2), the stress concentration around broken clusters can have a stronger and stronger effect on the evolution of the breaking process.

The average size of records must be a monotonically increasing function of the record rank at any degree of disorder qualitatively similar to the one presented in Fig. 4(a) for an infinite cutoff $\lambda = \infty$. More interesting behavior is expected for the average record lifetime $\langle m_k \rangle$ which is sensitive to the internal structure of the event sequence. It can be observed in Fig. 6(a) that for a low exponent $\mu = 0.1$, where the distribution of breaking thresholds decays slowly, the average lifetime $\langle m_k \rangle$ has a complex dependence on the upper cutoff of fibers' strength λ: Close to the phase boundary of perfectly brittle behavior $\lambda \to 0$ the $\langle m_k \rangle$ curves monotonically increase with the record rank k showing the slowdown of record breaking as fracture proceeds. The same behavior is observed in the opposite limit $\lambda \to \infty$, although, the curves saturate at significantly higher lifetime values which indicates that at higher disorder it takes longer to break a record. It is interesting to note that there is an intermediate cutoff range where the lifetime curves develop a well defined maximum at a characteristic record rank k^*. The result implies that the initial slowdown of record breaking is followed by an acceleration which sets on at the rank k^*. The slowdown is consistent with the IID behavior which indicates that in spite of the stress concentration around broken clusters the beginning of the fracture process is dominated by the strength disorder of fibers which gives rise to a high degree of stationarity of the avalanche sequence. Beyond the characteristic rank k^* the records rapidly follow each other due to the increase of the avalanche size as the system approaches global failure.

Fig. 6(b) demonstrates that the average number of records $\langle N_n \rangle$ exhibits the same two-phase behavior, i.e. the beginning of the fracture process is characterized by a logarithmic increase of the number of records consistent with Eq. (4) of IID sequences. However, at a characteristic event number n^* a faster increase sets on due to the rapid breaking of records after each other. The data analysis showed that the characteristic event index n^* is related to the record rank k^* as $n^* \approx n_{k^*}$, which provides a good approximation of the crackling event from which the avalanche activity gets more intensive. It follows that the start of accelerated record breaking n_{k^*} can be used to identify the onset of acceleration of the fracture process towards failure. This is illustrated in Fig. 6(b), where the value of n_{k^*} corresponding to the curve of $\lambda = 10^3$ with $k^* = 7$ is highlighted by the dashed lines. It can be observed that n_{k^*} falls close to n^* which is determined by fitting as the parameter D of Eq. (11) (explanation see later). Note that increasing the degree of strength disorder in Fig. 6(b) by increasing the cutoff strength λ, the slope of the $\langle N_n \rangle$ curves decrease which indicates that up to the same number of events less records emerge in the avalanche sequence. In the limit of very large cutoffs $\lambda \to \infty$ the acceleration regime gradually disappears and the curves converge to the case of disorder dominated fracture with a purely logarithmic increase of $\langle N_n \rangle$ as in Fig. 4(c).

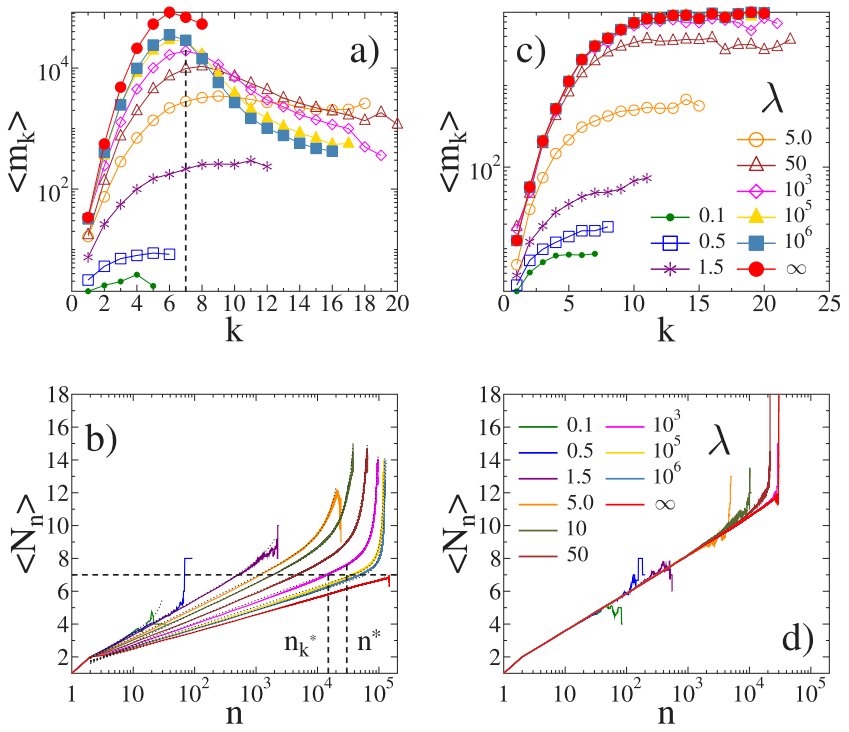

Fig. 6. Average lifetime $\langle m_k \rangle$ as a function of record rank k (top row) and the average number of records $\langle N_n \rangle$ that occurred up to the nth avalanche (bottom row) for two values of the disorder exponent $\mu = 0.1$ (a,b) and $\mu = 0.9$ (c,d). In (b) the thin dotted lines represent fits with the expression Eq. (11). In (a) the vertical dashed line highlights the record of rank $k^* = 7$ which has the maximum lifetime at $\lambda = 10^3$. In (b) the vertical and horizontal dashed lines guide the eye to identify the event index n_{k^*} for $k^* = 7$ which falls close to $n^* = D$, where the rapid increase of the $\langle N_n(\lambda = 10^3) \rangle$ curve sets on.

It can be observed in Figs. 6(c, d) for $\mu = 0.9$ that at higher strength exponents μ, i.e. at lower disorder, the accelerated record breaking is practically entirely missing. In spite of the fact that more records are generated the record lifetime $\langle m_k \rangle$ remains monotonous up to the highest rank (Fig. 6(c)), and the record number $\langle N_n \rangle$ is purely logarithmic for all values of the upper cutoff (Fig. 6(d)). In this disorder range the stress concentration dominates the fracture process which favors shorter avalanche sequences with a nearly stationary evolution. Note that the characteristic quantities of records such as their size Δ_r^k and lifetime m_k, furthermore the total number of records N_n that occurred up to a given event number n all have sample-to-sample fluctuations. The sample averaging is responsible for the fluctuations of the curves observed at high record ranks in Figs. 6(a,c) and at the end of the $\langle N_n \rangle$ curves in Figs. 6(b, d).

4. Significance of accelerated record breaking

To give a quantitative characterization of the effect of strength disorder on the acceleration of the RB process, first we fitted the $\langle N_n \rangle$ curves with the formula

$$\langle N_n \rangle = A + B \ln n + C e^{-(n/D)^{\xi}}, \tag{11}$$

which is the extension of the logarithmic increase of Eq. (4) with a term representing the acceleration by an exponential. It can be observed in Fig. 6(b) that Eq. (11) provides a reasonable fit of the simulation results. The parameters A, B, C, D, and ξ all depend on the disorder parameters: careful data analysis revealed that the values of A and C fluctuate in the ranges 0.5–1.0 and 0.6–0.8, respectively. Parameter B characterizes the rate of increase of the record number in the stationary logarithmic regime. It can be seen in Fig. 7 that its value monotonically decreases with increasing cutoff strength λ towards the limit value obtained when $\lambda = +\infty$. The value of D corresponds approximately to the event n^* of the sequence where the accelerated record breaking sets on $D \approx n^*$. It follows that when D is compared to the average value of the total number of events $\langle n_{max} \rangle$ in the fracture process, the extension of the accelerating regime preceding failure can be inferred. For small and very high disorder the ratio $D/\langle n_{max} \rangle$ falls close to 1 (see Fig. 7), indicating that acceleration is very short. However, in between a minimum emerges, where $D/\langle n_{max} \rangle \approx 0.5$, which implies that in the corresponding disorder range a significantly broad acceleration regime emerges. The rate of acceleration is controlled by the exponent ξ, whose value spans the range $1 < \xi < 7$ in Fig. 7. It is important to note that high exponent ξ is connected to high

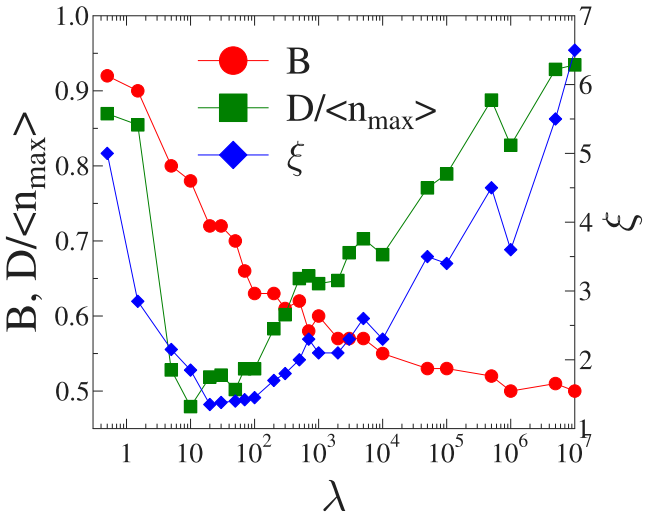

Fig. 7. The value of the parameters B, D and ξ of Eq. (11) obtained by fitting the $\langle N_n \rangle$ curves in Fig. 6(b). Parameter D is rescaled by the average value of the total number of avalanches $\langle n_{max} \rangle$, i.e. by the length of the avalanche sequence.

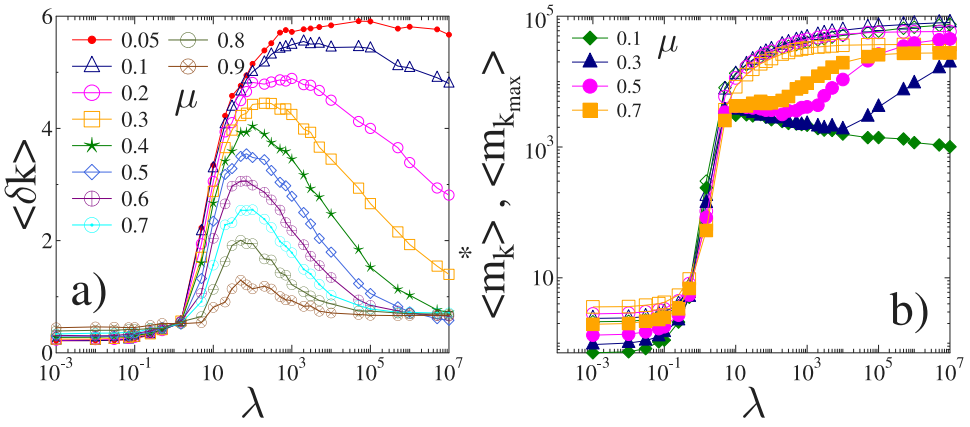

Fig. 8. (*a*) Average difference $\langle \delta k \rangle$ of the largest record rank and of the rank of the record with the highest lifetime $\langle \delta k \rangle = \langle k_{max} - k^* \rangle$ as a function of the cutoff strength λ for several values of the exponent μ. (*b*) Average value of the longest lifetime $\langle m_{k^*} \rangle$ (open symbols) and the average lifetime of the last record $m_{k_{max}}$ (filled symbols) as function of the cutoff strength λ for several values of the exponent μ.

values of $D/\langle n_{max} \rangle$, i.e. to short acceleration with a steep increase of $\langle N_n \rangle$. When failure is preceded by a broad accelerating regime the exponent has a minimum close to 1.

To obtain an overview of how the competition of strength and stress disorder affects the acceleration of the RB process, observed in the behavior of the average lifetime $\langle m_k \rangle$ in Fig. 6(*a*), we determined the average difference of the largest record rank k_{max} and of the rank k^* of the record with the longest lifetime

$$\langle \delta k \rangle = \left\langle k_{max} - k^* \right\rangle . \tag{12}$$

This quantity characterizes the significance of the accelerating regime of the RB process in the sense that a high value of $\langle \delta k \rangle$ implies a large number of records following the one of the longest lifetime. Fig. 8(*a*) presents $\langle \delta k \rangle$ as a function of the cutoff strength λ for several exponents μ. It can be seen that at each μ value the $\langle \delta k \rangle$ curves have a maximum which gets higher and broader and slightly shifts to the right as the strength exponent μ decreases. In agreement with the above findings, at the highest exponents $\mu = 0.8 - 0.9$ considered the value of the maximum falls between 1 and 2, which shows that practically no acceleration of the RB process can be detected. A significant acceleration with at least 5 records emerges only for sufficiently low exponents $\mu \lesssim 0.3$, where the strength distribution decays slowly. Far from the maximum, i.e. close to the phase boundary of perfect brittleness $\lambda \to 0$ and in the limit of very large cutoffs $\lambda \to \infty$, the value of $\langle \delta k \rangle$ falls below 1 due to the absence of accelerated breaking.

It is also a crucial question how quickly the records of the accelerating regime follow each other. To answer the question we compare the average lifetime of the last record $\left\langle m_{k_{max}} \right\rangle$ and the average of the longest lifetime $\langle m_{k^*} \rangle$ in the avalanche

sequence. It can be observed in Fig. 8(*b*) that for high values of μ the two curves practically coincide in agreement with the absence of acceleration. Large differences of $\langle m_{k^*} \rangle$ and $\langle m_{k_{max}} \rangle$ are obtained again at lower exponents $\mu \lesssim 0.3$ in well defined ranges of λ consistent with the behavior of $\langle \delta k \rangle$ in Fig. 8(*a*). The results clearly demonstrate that in an LLS FBM significant acceleration of the fracture process is limited to a well defined range of the strength disorder. When acceleration of the avalanche sequence is present the event index of the record with the longest lifetime can be used to identify the onset of acceleration which occurs sufficiently early before the ultimate failure of the bundle.

5. Discussion

Crackling noise accompanying the fracture of heterogeneous materials is one of the main information source about the microscopic dynamics of fracturing solids. Analyzing the time series of crackling events it is a crucial question if signatures of the imminent failure can be identified which could be used for forecasting. Here we investigated this problem in the framework of a fiber bundle model with localized load sharing where avalanches of fiber breakings emerging under a slowly increasing external load are analogous to crackling events of real systems. In the model the materials' disorder was represented by the random strength of fibers sampled from a power law distribution with a finite upper cutoff. The degree of the disorder of fibers' strength could be controlled by varying the exponent and the upper cutoff of the distribution. We studied how the competition of the quenched strength disorder and the evolving inhomogeneous stress field affects the structure of the sequence of breaking avalanches as the system approaches ultimate failure. Our analysis is based on the statistics of records which has proven powerful in the mean field limit of the model where the stress field remains always homogeneous [13].

We showed by computer simulations that for an infinite upper cutoff of fibers' strength the stress concentration around broken fibers has a minor effect on the fracture process: the statistics of record size avalanches proved to be completely consistent with the behavior of IID sequences, which implies a stationary evolution of the avalanche sequence up to global failure. When strength disorder is reduced by increasing the exponent of the threshold distribution, the avalanche activity and the record breaking process get intensified, however, the qualitative IID features remain valid.

For finite values of the cutoff strength the interplay of stress and strength disorders gives rise to a complex behavior: at high strength exponents, where the threshold distribution rapidly decays the evolution of the fracture process remains close to stationary, practically without any sign of acceleration towards failure. Simulations showed that this is the effect of stress concentration around cracks in the model which makes the response of the system more brittle. It means that failure is preceded by a small amount of damage in such a way that only small isolated cracks occur in the bundle without the opportunity to develop spatial correlation of avalanches. For slowly decaying distributions (small strength exponents) we pointed out the existence of a window of disorder where the lifetime of record size avalanches has a maximum: before the maximum the RB process slows down due to the stationarity of the avalanche sequence, however, beyond the maximum lifetime acceleration emerges. Acceleration of the RB process means that records rapidly follow each other with a decreasing lifetime due to the growing intensity of the breaking process. The characteristic record rank of the maximum lifetime can be used to identify the onset of acceleration of the fracture process. Outside this disorder range, close to the phase boundary of perfectly brittle behavior and in the limit of high cutoff strength, no acceleration is detected due to the dominating effect of stress concentration and of strength disorder, respectively.

To quantify the extension of the accelerating regime we determined the average difference $\langle \delta k \rangle$ of the largest record rank and of the rank of the record with the longest lifetime. Calculations showed that significant accelerated record breaking with at least five RB events is obtained solely for sufficiently small disorder exponents, where the threshold distribution of fibers decays slowly. The behavior of the average number of records, and the relation of the longest lifetime and the lifetime of the last record also confirmed this outcome. In Fig. 9 we compare the behavior of $\langle \delta k \rangle$ over the parameter plane of disorder $\mu - \varepsilon_{max}$ for LLS and ELS FBMs. It can be observed that the three-dimensional surfaces of the two models have qualitatively the same shape: there is an optimal amount of disorder where the broadest accelerating regime of the fracture process emerges. This occurs along the ridge of the two surfaces which are highlighted by the thick red lines. However, two important differences have to be emphasized: (*i*) for LLS FBMs the ridge shifts to higher strength cutoffs λ, indicating that due to stress concentrations around broken clusters, at a given exponent μ a higher degree of disorder, i.e. a higher value of λ is needed to stabilize the system. (*ii*) The LLS ridge is significantly lower than its ELS counterpart, i.e. the accelerating regime has a narrower extension in the presence of stress concentrations. In ELS FBMs the stress field is always homogeneous over the intact fibers so that the fracture process is driven by the disordered strength of fibers and the gradually increasing stress. Our calculations showed that stress localization around cracks makes overloaded fibers more prone to breaking, which prevents the emergence of long accelerating record breaking sequences close to failure. The onset of acceleration of the fracture process detected with the acceleration of record breaking may be exploited to obtain an early signal of the imminent catastrophic failure of the system. However, when stress concentrations are present, this signal occurs significantly closer to failure than in a homogeneous stress field.

Our study is based on computer simulations of the localized load sharing fiber bundle model with a system size $L = 401$, which makes it feasible to generate a reasonable number of samples for averaging at each parameter set considered. The disordered strength of fibers gives rise to a statistical size effect of the ultimate strength of the bundle which has been explored in the ELS limit of our model [28]. This size effect is expected to show up also in LLS bundles affecting the record statistics of avalanches, as well, which will be explored in a forthcoming publication.

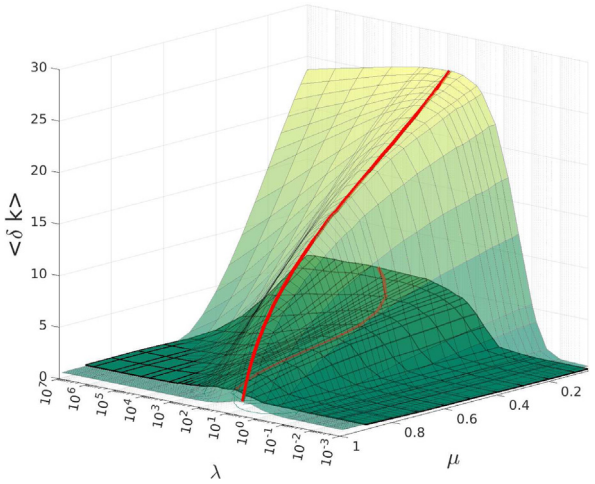

Fig. 9. Average difference $\langle \delta k \rangle$ of the largest record rank and of the rank of the record with the highest lifetime $\langle \delta k \rangle = \langle k_{max} - k^* \rangle$ obtained from computer simulations over the entire parameter plane. Dark green indicates the 3D surface obtained for LLS, while the yellow–light green color shows the ELS counterpart of the system. The continuous red lines highlight the ridge of the two surfaces.

CRediT authorship contribution statement

Viktória Kádár: Software development, Computer simulations, Data evaluation. **Zsuzsa Danku:** Software development, Computer simulations, Data evaluation. **Gergő Pál:** Computer simulations, Visualization, Investigation. **Ferenc Kun:** Conceptualization, Methodology, Writing – review & editing, Supervision.

Declaration of competing interest

The authors declare the following financial interests/personal relationships which may be considered as potential competing interests: Ferenc Kun reports financial support was provided by National Research, Development and Innovation Fund of Hungary, financed under the K-16 funding scheme Project no. K 119967. Zsuzsa Danku reports financial support was provided by National Research, Development and Innovation Fund of Hungary, financed under the 2020-4.1.1-TKP2020 funding scheme. Viktoria Kadar reports financial support was provided by UNKP-20-3 New National Excellence Program of the Ministry for Innovation and Technology from the source of the National Research, Development and Innovation Fund.

Acknowledgments

The work is supported by the EFOP-3.6.1-16-2016-00022 project. This research was supported by the National Research, Development and Innovation Fund of Hungary, financed under the K-16 funding scheme Project no. K 119967. Project no. TKP2020-NKA-04 has been implemented with the support provided from the National Research, Development and Innovation Fund of Hungary, financed under the 2020–4.1.1-TKP2020 funding scheme. Supported by the ÚNKP-20-3 New National Excellence Program of the Ministry for Innovation and Technology from the source of the National Research, Development and Innovation Fund, Hungary.

References

[1] A. Guarino, A. Garcimartin, S. Ciliberto, An experimental test of the critical behaviour of fracture precursors, Eur. Phys. J. B 6 (1998) 13–24.
[2] J. Baró, A. Corral, X. Illa, A. Planes, E.K.H. Salje, W. Schranz, D.E. Soto-Parra, E. Vives, Statistical similarity between the compression of a porous material and earthquakes, Phys. Rev. Lett. 110 (2013) 088702.
[3] P.O. Castillo-Villa, J. Baró, A. Planes, E.K.H. Salje, P. Sellappan, W.M. Kriven, E. Vives, Crackling noise during failure of alumina under compression: the effect of porosity, J. Phys.: Condens. Matter 25 (29) (2013) 292202.
[4] Y. Zhao, H. Liu, K. Xie, E.K. Salje, X. Jiang, Avalanches in compressed sandstone: Crackling noise under confinement, Crystals 9 (11).
[5] E.K. Salje, K.A. Dahmen, Crackling noise in disordered materials, Annu. Rev. Condens. Matter Phys. 5 (1) (2014) 233–254.
[6] S. Hao, C. Liu, C. Lu, D. Elsworth, A relation to predict the failure of materials and potential application to volcanic eruptions and landslides, Sci. Rep. 6 (2016) 27877.
[7] J.J. McGuire, M.S. Boettcher, T.H. Jordan, Foreshock sequences and short-term earthquake predictability on east pacific rise transform faults, Nature 434 (2005) 457.
[8] D. Sornette, Predictability of catastrophic events: Material rupture, earthquakes, turbulence, financial crashes, and human birth, Proc. Natl. Acad. Sci. USA 99 (2002) 2522–2529.

[9] G. Niccolini, A. Carpinteri, G. Lacidogna, A. Manuello, Acoustic emission monitoring of the syracuse athena temple: Scale invariance in the timing of ruptures, Phys. Rev. Lett. 106 (2011) 108503.
[10] J. Vasseur, F.B. Wadsworth, Y. Lavallée, A.F. Bell, I.G. Main, D.B. Dingwell, Heterogeneity: The key to failure forecasting, Sci. Rep. 5 (2015) 13259.
[11] B. Voight, A relation to describe rate-dependent material failure, Science 243 (4888) (1989) 200–203.
[12] S.-W. Hao, F. Rong, L. Ming-Fu, H.-Y. Wang, M.-F. Xia, K. Fu-Jiu, Y.-L. Bai, Power-law singularity as a possible catastrophe warning observed in rock experiments, Int. J. Rock Mech. Min. Sci. 60 (2013) 253–262.
[13] V. Kádár, G. Pál, F. Kun, Record statistics of bursts signals the onset of acceleration towards failure, Sci. Rep. 10 (2020) 2508.
[14] G. Wergen, Records in stochastic processes—theory and applications, J. Phys. A 46 (22) (2013) 223001.
[15] B.C. Arnold, N. Balakrishnan, H.N. Nagaraja, Records, John Wiley & Sons, 2011.
[16] X. Jiang, H. Liu, I.G. Main, E.K.H. Salje, Predicting mining collapse: Superjerks and the appearance of record-breaking events in coal as collapse precursors, Phys. Rev. E 96 (2017) 023004.
[17] F. Kun, F. Raischel, R.C. Hidalgo, H.J. Herrmann, Extensions of fiber bundle models, in: P. Bhattacharyya, B.K. Chakrabarti (Eds.), Modelling Critical and Catastrophic Phenomena in Geoscience: A Statistical Physics Approach, in: Lecture Notes in Physics, Springer-Verlag, Berlin Heidelberg New York, 2006, pp. 57–92.
[18] A. Hansen, P. Hemmer, S. Pradhan, The fiber bundle model: Modeling failure in materials, in: Statistical Physics of Fracture and Breakdown, Wiley, 2015.
[19] S. Pradhan, J.T. Kjellstadli, A. Hansen, Variation of elastic energy shows reliable signal of upcoming catastrophic failure, Front. Phys. 7 (2019) 106.
[20] Z. Halász, I. Kállai, F. Kun, Stick–slip dynamics in fiber bundle models with variable stiffness and slip number, Front. Phys. 9 (2021) 8.
[21] M. Kloster, A. Hansen, P.C. Hemmer, Burst avalanches in solvable models of fibrous materials, Phys. Rev. E 56 (1997) 2615–2625.
[22] R.C. Hidalgo, F. Kun, K. Kovács, I. Pagonabarraga, Avalanche dynamics of fiber bundle models, Phys. Rev. E 80 (2009) 051108.
[23] S. Zapperi, P. Ray, H.E. Stanley, A. Vespignani, Analysis of damage clusters in fracture processes, Physica A 270 (1999) 57.
[24] G. Dill-Langer, R.C. Hidalgo, F. Kun, Y. Moreno, S. Aicher, H.J. Herrmann, Size dependency of tension strength in natural fiber composites, Physica A 325 (2003) 547–560.
[25] F. Kun, S. Zapperi, H.J. Herrmann, Damage in fiber bundle models, Eur. Phys. J. B 17 (2000) 269.
[26] S. Sinha, S. Roy, A. Hansen, Crack localization and the interplay between stress enhancement and thermal noise, Physica A 569 (2021) 125782.
[27] Z. Danku, F. Kun, Fracture process of a fiber bundle with strong disorder, J. Stat. Mech.: Theor. Exp. 2016 (7) (2016) 073211.
[28] V. Kádár, Z. Danku, F. Kun, Size scaling of failure strength with fat-tailed disorder in a fiber bundle model, Phys. Rev. E 96 (2017) 033001.
[29] V. Kádár, F. Kun, System-size-dependent avalanche statistics in the limit of high disorder, Phys. Rev. E 100 (2019) 053001.
[30] A. Hansen, E.L. Hinrichsen, S. Roux, Scale-invariant disorder in fracture and related breakdown phenomena, Phys. Rev. B 43 (1991) 665–678.
[31] S. Sinha, S. Roy, A. Hansen, Phase transitions and correlations in fracture processes where disorder and stress compete, Phys. Rev. Res. 2 (2020) 043108.
[32] G. Pál, F. Raischel, S. Lennartz-Sassinek, F. Kun, I.G. Main, Record-breaking events during the compressive failure of porous materials, Phys. Rev. E 93 (2016) 033006.
[33] J. Davidsen, P. Grassberger, M. Paczuski, Earthquake recurrence as a record breaking process, Geophys. Res. Lett. 33 (11) l11304.
[34] G.F. Nataf, P.O. Castillo-Villa, P. Sellappan, W.M. Kriven, E. Vives, A. Planes, E.K.H. Salje, Predicting failure: acoustic emission of berlinite under compression, J. Phys.: Condens. Matter 26 (27) (2014) 275401.
[35] G. Wergen, J. Krug, Record-breaking temperatures reveal a warming climate, Europhys. Lett. 92 (3) (2010) 30008.